Journal of Electrochemistry

Volume 25
Issue 2 *Special Issue: Electrochemical Analysis and Sensing (I)*

2019-04-28

High-Efficiency Nitrite Sensor Based on CoP Nanowire Array

Fu-ling ZHOU

Xiao-li XIONG
College of Chemistry and Material Science, Sichuan Normal University,Chengdu 610068, Sichuan, China;, xiongxiaoli2000@163.com

Xu-ping SUN
Institute of Fundamental and Frontier Sciences, University of Electronic Science and Technology of China,Chengdu 610054, Sichuan, China;, xpsun@uestc.edu.cn

DOI: 10.13208/j.electrochem.181055 **Artical ID**:1006-3471(2019)02-0252-08
Cite this: *J. Electrochem*. **2019**, *25*(2): 252-259 **Http**://electrochem.xmu.edu.cn

基于CoP纳米阵列的亚硝酸根传感器的研究

周福玲[1,2],熊小莉[2*],孙旭平[1*]
(1. 电子科技大学基础与前沿研究院, 四川 成都 610054;
2. 四川师范大学化学与材料科学学院, 四川 成都 610068)

摘要: 亚硝酸盐对环境和人体健康有着不利的影响,人体长期食用含大量亚硝酸盐的食物有致癌的风险,对亚硝酸盐的分析和检测是非常重要的. 开发高效的电催化剂,从而实现高灵敏度和高选择性的亚硝酸盐检测具有十分重要的意义. 作者通过先水热再低温磷化获得了磷化钴纳米阵列 (CoP/TM). 电化学测试结果表明, 所构建的CoP/TM电极对亚硝酸盐的还原具有高效的催化作用,线性检测范围为1.0 μmol·L^{-1}到1.0 mmol·L^{-1},检测下限为18 nmol·L^{-1}(*S*/*N*=3),响应灵敏度为17781 μA·(mmol·L^{-1})$^{-1}$·cm^{-2},响应时间小于3 s,选择性良好.

关键词: 磷化钴;纳米阵列;亚硝酸钠;电化学;传感器
中图分类号: O646 **文献标识码**: A

亚硝酸盐作为食品防腐剂和肥料的重要原料,也是癌基因N-亚硝胺形成的基本前驱体,在环境中广泛存在,受到全世界的关注[1-4],准确监控亚硝酸盐对公共卫生、环境和食品工业安全具有非常重要的意义. 亚硝酸根的分析检测方法包括荧光法、化学发光法、毛细管电泳法和色谱法. 但这些方法所用设备昂贵、检测过程繁琐、耗时长,进一步应用受限,而电化学方法可以提供灵敏可靠,成本较低,可以实现对亚硝酸根实时快速的检测[10-11].

作为一个理想的电化学传感催化剂应该具有以下3点优势:1) 良好快速的电子传输能力;2)丰富的活性位点;3)易于接触目标分子. 过渡金属磷化物(TMPs)是一类重要的类金属化合物[12-13],具有极好的金属性能和良好的导电性, 对提高电催化性能十分有利[14,16]. 在众多过渡金属磷化物中,磷化钴(CoP)因其良好的电催化性能和电化学氧化还原活性以及化学稳定性而被广泛应用于非酶过氧化氢传感以及葡萄糖传感[17-18]. 然而,CoP在基于阴极催化还原的电化学亚硝酸盐检测方面的应用还尚未见报道.

本文首次报道了以负载在钛网上的磷化钴纳米线阵列(CoP/TM)作为催化电极,在中性条件下对亚硝酸盐电还原的催化响应, 构建了一种高选择性的新颖的亚硝酸盐电化学非酶传感方法. 该CoP/TM电极具有优良的传感性能, 响应灵敏度为11781 μA·(mmol·L^{-1})$^{-1}$·cm^{-2}, 线性响应范围为1 μmol·L^{-1} ~ 5.0 mmol·L^{-1},检测下限低至18 nmol·L^{-1}(*S*/*N*=3),响应时间小于 3 s,运用于实际样品中的亚硝酸根的检测,结果满意.

1 实 验

1.1 试剂与仪器

次磷酸钠(NaH_2PO_2)购自阿拉丁有限公司(上海,中国). 六水合硝酸钴($Co(NO_3)_2·6H_2O$),氟化铵(NH_4F)和尿素(urea)购自北京化工公司. 钛网(TM)由河北省衡水市杭徐过滤旗店提供. 所有化学试剂均未经过任何纯化处理,直接使用,实验用水为Millipore系统处理的超纯二次去离子水(电阻值为18.2 MΩ·cm,25 ℃).

电化学数据由上海辰华CHI 660E电化学工作站采集得到;扫描电镜照片(SEM)由XL30场发射扫描电镜显微镜仪采集;X-射线衍射谱图(XRD)由日立公司RigakuD/MAX 2550 X射线衍射仪采集,用Cu做射线源(λ =1.5418 Å);X- 射线光电子能谱(XPS)测定采用ESCALAB-MKII 250能谱仪(VG Co., U.K.),Mg K_α X- 射线源激发,在常温下采集实验数据; 透射电镜 (TEM) 采用日本的HITACHI

收稿日期:2019-01-02, 修订日期:2019-01-26 * 通讯作者, Tel: (86-28)84760802, E-mail: xiongxiaoli2000@163.com;Tel: (86)17716153137,E-mail: xpsun@uestc.edu.cn
国家自然科学基金项目(No. 21575137)资助

H-8100电子显微镜,加速电压为200 kV.

1.2 实验方法或样品的制备和测试

1)磷化三钴纳米线阵列的制备方法

钛网首先用稀盐酸和乙醇清洗几次，以去除表面的杂质. 在室温下,0.685 g六水合硝酸钴、0.685 g氟化铵和3.0 g尿素溶解在36 mL蒸馏水中,搅拌成透明均匀的溶液. 将溶液和洗净的钛网一同转移到40 mL聚四氟乙烯高压釜中,密封,100 °C下保持8 h,自然冷却到室温,得到前驱材料. 然后将盛有1.0 g次磷酸钠的瓷舟置于管式炉中,将制备

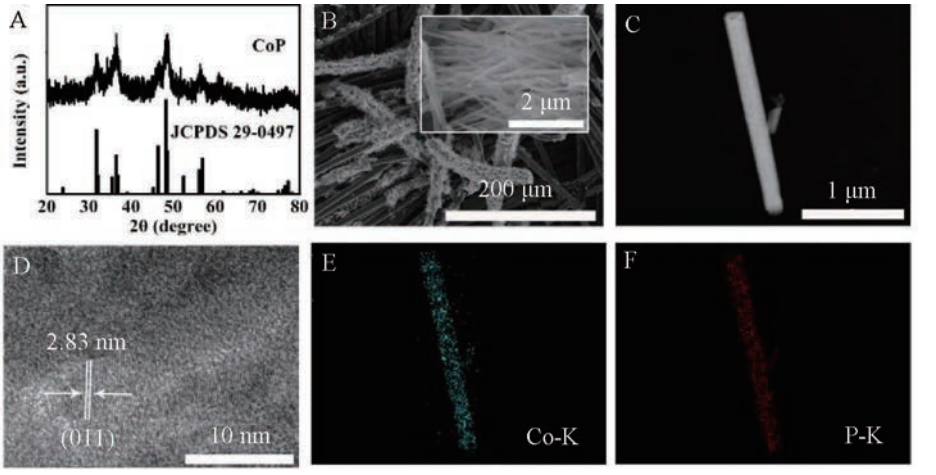

图1 (A) CoP的XRD图谱. (B) CoP的低倍和高倍SEM照片. (C)-(D)CoP纳米线的TEM照片和HRTEM照片. (E)-(F) CoP的Co和P的EDX元素映射图像.

Fig. 1 (A) XRD pattern of CoP. (B) Low- and (inset) highmagnification SEM images of CoP. (C) TEM and (D) HRTEM images of CoP nanowire. (E) and (F) EDX elemental mapping images for Co (E) and P (F) of CoP/TM.

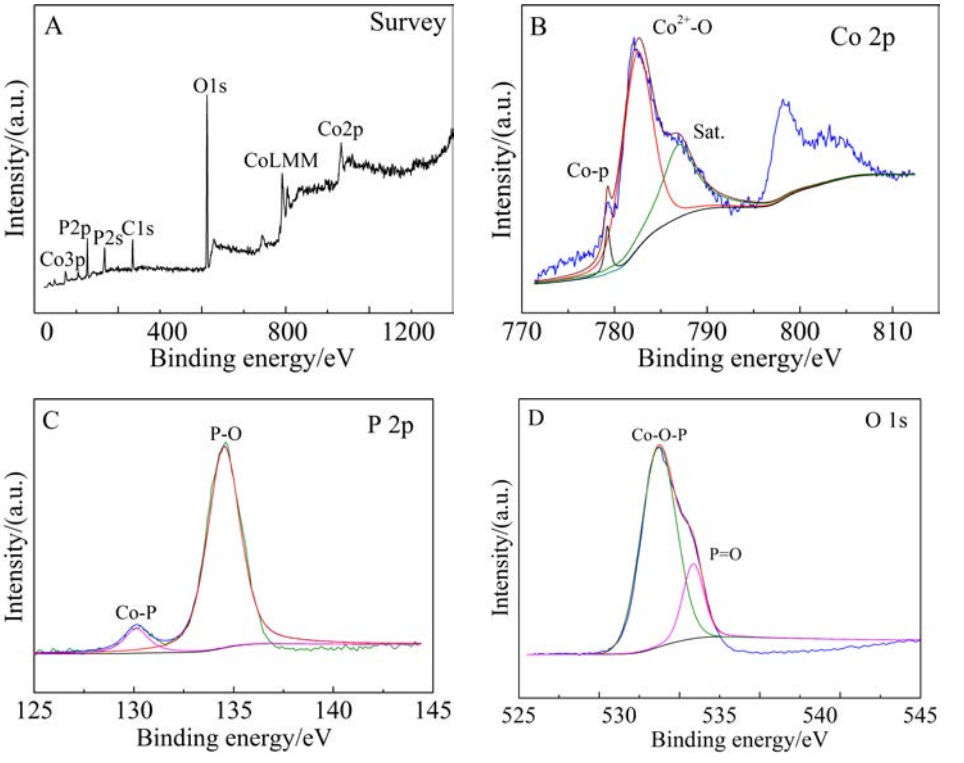

图2 (A) CoP的XPS光谱(B) Co 2p, (C) P 2p和(D)O 1s

Fig. 2 (A) XPS survey spectrum of CoP. XPS spectra of CoP in the (B) Co 2p, (C) P 2p, and (D) O 1s regions

好的前驱材料放置在另一瓷舟中，将用锡箔纸包好的双瓷舟置于管式炉温区中心的区域，排净炉内空气，在氩气气氛保护下，管式炉中心温度以2 °C·min^{-1}升至300 °C，保温2 h. 反应结束后自然冷却至室温，取出反应后的样品即为CoP/TM.

2）电化学测试方法

所有的电化学数据均由上海辰华CHI 660E电化学工作站上采集. 所制备的电极的电化学性能是通过经典的三电极体系测试，新制的CoP/TM直接作为工作电极，Ag/AgCl电极作为参比电极，石墨棒作为对电极.

2　结果与讨论

2.1　CoP/TM的结构和形貌表征

图1A是CoP/TM的XRD图谱，其特征衍射峰与磷化钴（JCPDS No. 29-0497[19]）吻合. 图1B为CoP/TM的SEM照片，从图中可以看到，CoP/TM纳米线阵列均匀的覆盖在钛网上. 图1C为CoP纳米线的TEM照片. 图1D为CoP纳米线的HRTEM照片，结果显示该材料具有良好的晶格条纹，其晶面间距为0.283 nm，对应CoP相的（011）晶面[20]. EDX元素映射分析证实了Co和P元素均匀分布在纳米阵列中（图1E和F）.

图2A为CoP纳米线的XPS能谱，由于产品的污染/表面氧化，CoP的XPS呈现出Co、P和O的信号峰. 图2B是Co 2p的高分辨率XPS光谱，在778.1 eV的峰可归因于CoP中Co $2p_{3/2}$的结合能，而在782.0 eV的峰与787.0 eV的峰表明CoP/TM中Co^{2+}的存在. 如图2C所示，高分辨P 2p谱中129.5和

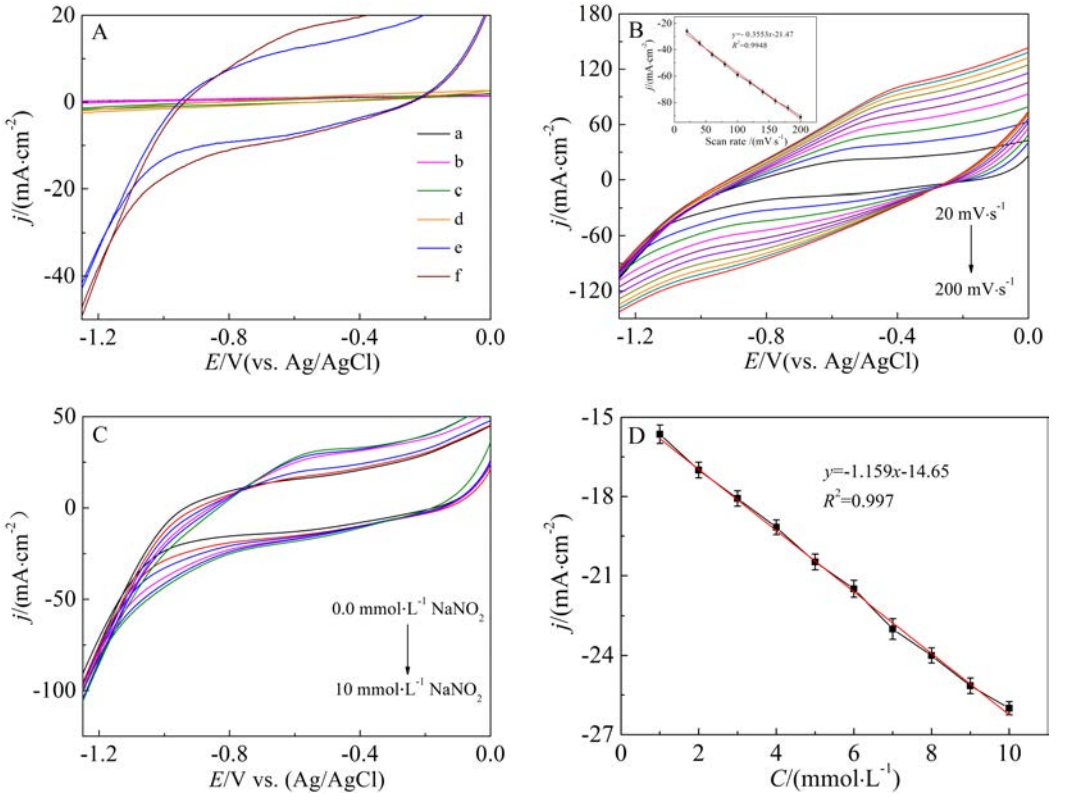

图3　(A) 空白TM (a, b)，前驱材料 (c, d) 和CoP/TM (e, f) 在0.1 mol·L^{-1} Na_2SO_4溶液中的CV，不含(a, c, e) 和含有1.0 mmol·L^{-1} $NaNO_2$的存在(b, d, f) (扫描速率：30 mV·s^{-1}). (B) CoP/TM在0.1 mol·L^{-1} Na_2SO_4和1.0 mmol·L^{-1} $NaNO_2$中的扫描速率为20至200 mV·s^{-1}的CV（插入的小图为相应的校准曲线）. (C) CoP/TM在0.1 mol·L^{-1} Na_2SO_4中的CV曲线，$NaNO_2$浓度：0, 2, 4, 6, 8和10 mmol·L^{-1}（从内到外），扫描速率为30 mV·s^{-1}. (D) 相应的校准曲线.

Fig. 3　(A) CVs of blank TM (a, b), precursor material (c, d) and CoP/TM (e, f) in 0.1 mol·L^{-1} Na_2SO_4 solution in the absence (a, c, e) and presence (b, d, f) of 1 mmol·L^{-1} $NaNO_2$ (scan rate: 30 mV·s^{-1}). (B) CVs for CoP/TM in 0.1 mol·L^{-1} Na_2SO_4 and 1.0 mmol·L^{-1} $NaNO_2$ solutions at scan rates from 20 to 200 mV·s^{-1} (inset: the corresponding calibration curve). (C) CV curves for CoP/TM in 0.1 mol·L^{-1} Na_2SO_4 containing different $NaNO_2$ concentrations: 0, 2, 4, 6, 8 and 10 mmol·L^{-1} (from inner to outer) at a scan rate of 30 mV·s^{-1}. (D) Corresponding calibration curve.

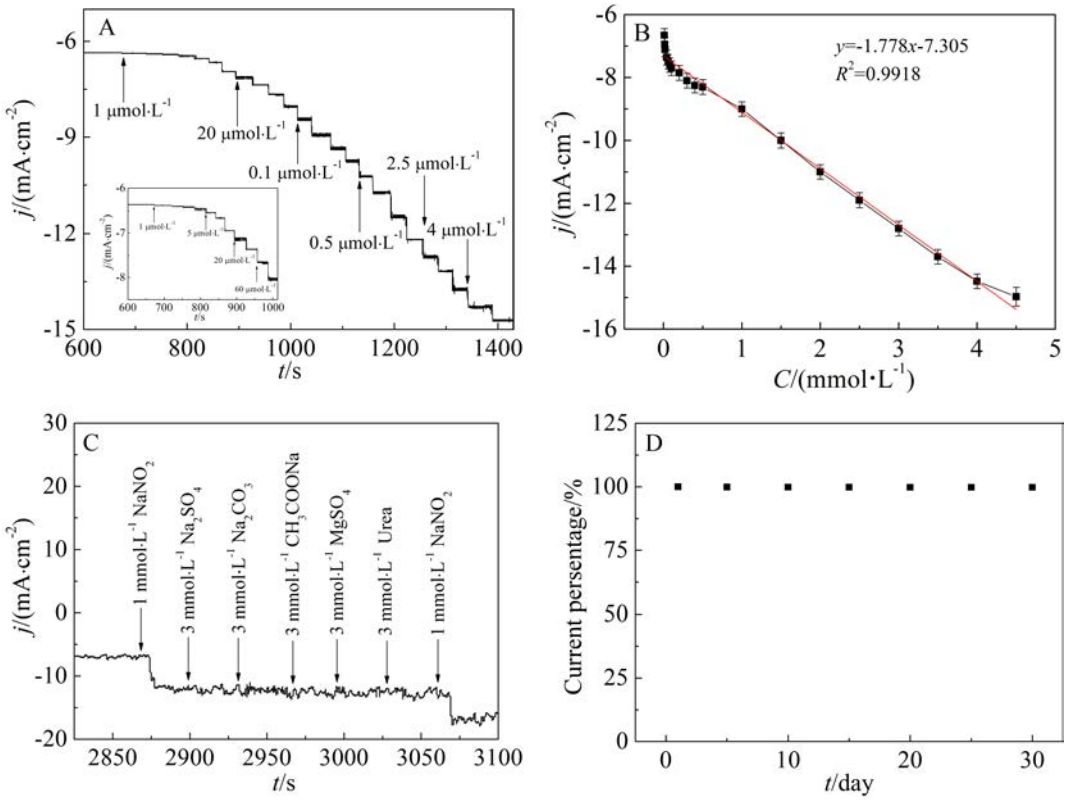

图4 (A) 在- 0.85 V下CoP/TM在0.1 mol·L-1 Na_2SO_4溶液中连续加入$NaNO_2$后的安培响应. (B) 在- 0.85 V下CoP/TM在0.1 mol·L-1 Na_2SO_4中连续添加$NaNO_2$时相应的校准曲线. (C) 在-0.85 V下在0.1 mol·L-1 Na_2SO_4中,连续加入1.0 mmol·L-1 $NaNO_2$, 3.0 mmol·L-1 Na_2SO_4, 3.0 mmol·L-1 Na_2CO_3, 3.0 mmol·L-1 NaAc, 3.0 mmol·L-1 $MgSO_4$, 3.0 mmol·L-1 Na_2SO_4和1.0 mmol·L-1 $NaNO_2$,CoP/TM的安培响应. (D) 在0.1 mol·L-1 Na_2SO_4中,CoP/TM对1 mmol·L-1 $NaNO_2$的响应电流变化30天(扫描速率: 30 mV·s-1).

Fig. 4 (A) Amperometric responses of CoP/TM upon successive additions of $NaNO_2$ in 0.1 mol·L-1 Na_2SO_4 solution at -0.85 V. (B) The corresponding calibration curves of CoP/TM to successive additions of $NaNO_2$ at -0.85 V in 0.1 mol·L-1 Na_2SO_4. (C) Amperometric responses of CoP/TM to the successive additions of 1.0 mmol·L-1 $NaNO_2$, 3.0 mmol·L-1 Na_2SO_4, 3.0 mmol·L-1 Na_2CO_3, 3.0 mmol·L-1 NaAc, 3.0 mmol·L-1 $MgSO_4$, 3.0 mmol·L-1 Na_2SO_4, and 1.0 mmol·L-1 $NaNO_2$ at -0.85 V in 0.1 mol·L-1 Na_2SO_4. (D) The variation in the response current of CoP/TM toward 1 mmol·L-1 $NaNO_2$ in 0.1 mol·L-1 Na_2SO_4 for 30 days (scan rate: 30 mV·s-1)

134.2 eV的两个峰可归因于纳米阵列中的磷化物和磷酸盐;O 1s光谱(图2D)显示氧化态钴和磷的存在[21].

2.2 CoP/TM检测亚硝酸根的电化学性能测试

采用石墨棒作为对电极,银/氯化银作为参比电极,CoP/TM作为工作电极, 考察了CoP/TM电极对$NaNO_2$还原反应的电催化性能. 图3A为在0.1 mol·L-1硫酸钠溶液中,空白钛网(TM)、前驱材料和CoP/TM对不含亚硝酸钠(a, c, e)和含1.0 mmol·L-1亚硝酸钠(b, d, f)的响应(扫描电位范围为0.0到-1.25 V,扫描速率为30 mV·s-1). 如图所示, 在没有加入亚硝酸钠时,TM和前驱没有还原峰(曲线a和曲线c),加入1.0 mmol·L-1亚硝酸钠后TM和前驱材料也基本没有催化电流响应 (曲线b和曲线d). 形成显著对比的是,在没有加入亚硝酸钠时,CoP/TM表现出明显的还原峰(曲线e),在加入1.0 mmol·L-1亚硝酸钠后,阴极还原峰值电流明显增加(曲线f),这也说明TM以及前驱材料不参与电催化反应,亚硝酸钠的电催化还原是由负载在TM上的CoP纳米结构实现的. 由图可知,在-0.85 V左右阴极峰电流密度达到最大值, 故本工作选择-0.85 V作为之后检测亚硝酸根的电位.

为进一步了解CoP/TM电极的电化学行为,作

者研究了CoP/TM电极在不同扫描速率10 ~ 200 mV·s^{-1}下的循环伏安行为,如图3B所示,峰电流随着扫描速率的增加而增加，且峰电流与扫描速率成正比，表明该过程涉及的电子转移反应是一个吸附控制过程. 图3C为CoP/TM在不同亚硝酸钠浓度下的电流响应,结果表明,还原电流随着亚硝酸钠浓度的增加而增加，表明该电极可以高效还原亚硝酸钠. 相应的校准曲线进一步表明（图3D)，阴极峰电流密度随着亚硝酸钠浓度的增加而线性增加.

作者将工作电位定为-0.85 V，在持续搅拌的条件下,向0.1 mol·L^{-1} Na_2SO_4溶液中连续加入亚硝酸钠来测量CoP/TM对亚硝酸盐的安培响应（图4A). 如图所示,加入亚硝酸盐后,催化还原电流急剧地增加到最大稳态电流值并且在3 s内达到稳态电流密度，表明该电极可以实现对亚硝酸盐的快速电流响应. 根据图4B亚硝酸盐检测校正曲线可知，其线性范围为1.0 μmol·L^{-1} ~ 1.0 mmol·L^{-1},灵敏度为1778 μA·(mmol·L^{-1})$^{-1}$·cm^{-2}. 在信噪比等于3时(*S*/*N*=3),检出限(LOD)低至18 nmol·L^{-1}. 以上这些性能优于大多数报道过的基于非贵金属电催化剂的亚硝酸盐传感器(表1).

2.3 CoP/TM在中性条件下的抗干扰能力、重现性和稳定性

抗干扰能力是传感器最重要的的分析能力之一. 如图4C所示，当3倍于亚硝酸盐浓度的干扰物质(硫酸钠、碳酸钠、醋酸钠、硫酸镁和尿素)加入到电解质溶液时，对亚硝酸盐检测没有产生明显干扰,这表明CoP/TM对亚硝酸盐具有优异的选择性.

作者研究了CoP/TM电极作为亚硝酸盐传感器的重现性和稳定性. 通过使用5个CoP/TM电极测量还原亚硝酸盐的还原电流响应来鉴别该传感器的重现性. 阴极峰电流密度的相对标准偏差(RSD)仅为4.8%,表明重现性良好. 传感器的长期稳定性是实际检测应用的关键因素. 因此,将CoP/TM电极在室温下暴露于空气中一个月之后,CoP/TM电极对1.0 mmol·L^{-1}亚硝酸盐的电流响应仅下降了11.3%,表明电极具有良好的稳定性(图4D).

2.4 CoP/TM实际样品检测

为评估该传感方法在实际应用中的可靠性,将电极用于检测河水和自来水中的亚硝酸盐含量. 结果如图所示,随着自来水(图5A)和河水(图5C)中亚硝酸盐浓度的增加，还原峰值电流密度增加.

表1 CoP/TM检测亚硝酸盐的性能与已报道的电催化剂比较

Tab. 1 Comparison of the CoP/TM performances for nitrite with the reported electrocatalysts

Catalyst	Sensitivity/ (μA·(mmol·L^{-1})$^{-1}$·cm^{-2})	Linear range/ (mmol·L^{-1})	LOD/(μmol·L^{-1})	Ref.
CoP/TM	1778	0.001~1.0	0.018	This work
Pd/SWCNT	417 192	2~238 283~1230	0.25	[22]
Fe_2O_3/rGO	204	0.05~780	0.015	[23]
Cu-NDs/RGO	214	125~13000	0.4	[24]
nano-Au/Ch	0.354	0.4~750	0.1	[25]
rGO-Co_3O_4@Pt	0.026	10~650	1.73	[26]
AuNPs-ERGO	5.38	Up to 3.38	0.133	[27]
f-ZnO@rFGO	/	10~8000	33	[28]
Co_3O_4/RGO	29.5	1~380	0.14	[29]
CuO/NiO	282.72	0.001~5	0.5	[30]
Pt/CoO	901.4 408.5	0.0002~3.67 3.67~23.7	0.067	[31]
$NiPc(OH)_4$/PEO	/	0.1~5300	0.0522	[32]
CR-GO	267	8.9~167	1	[33]

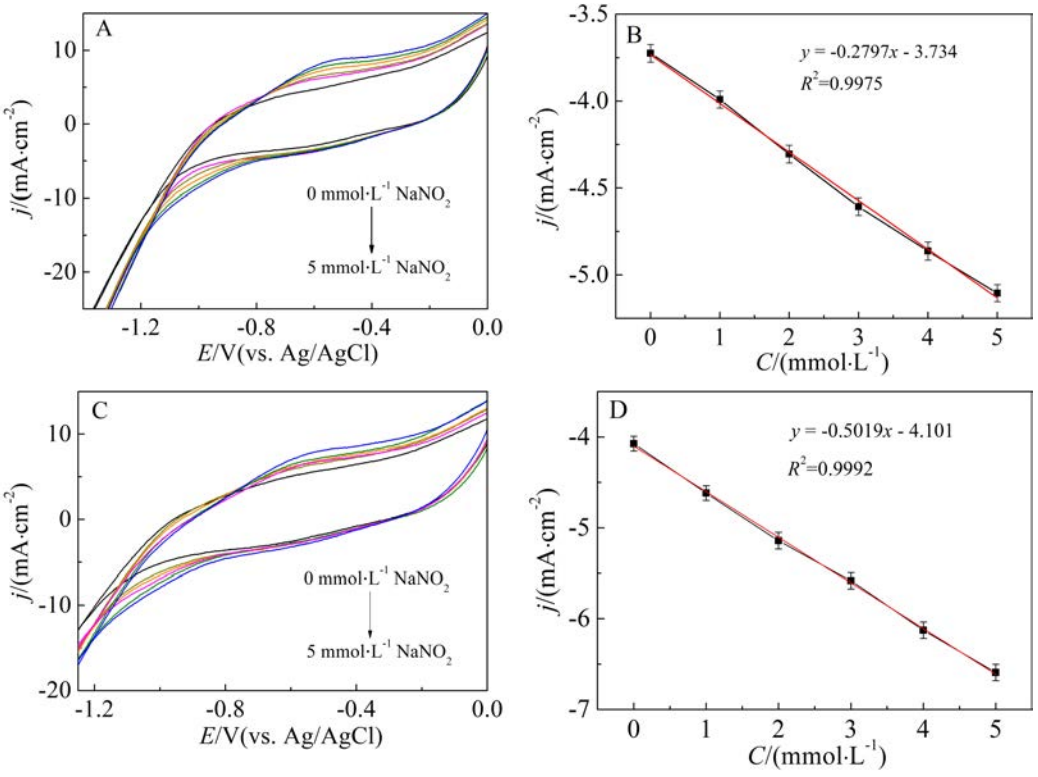

图5 (A, C) 在0.1 mol·L^{-1} Na_2SO_4中,电压为-0.85 V,当$NaNO_2$浓度从内到外依次为0、1、2、3、4和5 mmol·L^{-1}时,自来水和河水中CoP/TM的CV曲线(扫描速率:30 mV·s^{-1}). (B,D)分别对应河水和自来水的校准曲线.

Fig. 5 (A, C) CV curves of CoP/TM in tap water and river water at -0.85 V in 0.1 mol·L^{-1} Na_2SO_4 with the presence of varied $NaNO_2$ concentrations: 0, 1, 2, 3, 4, and 5 mmol·L^{-1} from inner to outer (scan rate: 30 mV·s^{-1}). (B, D) Corresponding calibration curves of river water and tap water.

由图5B、D可知，在0.0 mmol·L^{-1} ~ 5.0 mmol·L^{-1}范围内，校准曲线随着加入的亚硝酸盐的增加而线性增加. 这些结果表明,CoP/TM电极可用于实际样品中亚硝酸盐的检测.

3 结　论

本文采用水热法及低温磷化法在钛网上原位制备了CoP/TM纳米阵列材料,以此作为工作电极构建非酶亚硝酸盐的电化学传感器，得到了优异的电化学传感性能，该传感器灵敏度高，稳定性好，运用于实际样品的检测，取得了满意的结果. 该研究不仅提供了一个性能优异的电化学亚硝酸根非酶传感器电极材料的制备方法，还提供了一个基于过渡金属磷化物纳米阵列材料的电化学传感新思路.

参考文献(References):

[1] Manea F, Remes A, Radovan C, et al. Simultaneous electrochemical determination of nitrate and nitrite in aqueous solution using Ag-doped zeolite-expanded graphite-epoxy electrode[J]. Talanta, 2010, 83(1): 66-71.

[2] Braman R S, Hendrix S A. Nanogram nitrite and nitrate determination in environmental and biological materials by vanadium(III) reduction with chemiluminescence detection[J]. Analytical Chemistry, 1989, 61(24): 2715-2718.

[3] Guadagnini L, Tonelli D. Carbon electrodes unmodified and decorated with silver nanoparticles for the determination of nitrite, nitrate and iodate[J]. Sensors and Actuators B: Chemical, 2013, 188: 806-814.

[4] Panchompoo J, Compton R G. Electrochemical detection of ammonia in aqueous solution using fluorescamine: comparison of fluorometric versus voltammetric analysis [J]. Journal of Electrochemistry(电化学), 2012, 18(5): 437-449.

[5] Okafor P N, Ogbonna U I. Nitrate and nitrite contamination of water sources and fruit juices marketed in South-Eastern Nigeria[J]. Journal of Food Composition and Analysis, 2003, 16(2): 213-218.

[6] Akyüz M, Ata S. Determination of low level nitrite and ni-

trate in biological, food and environmental samples by gas chromatography-mass spectrometry and liquid chromatography with fluorescence detection[J]. Talanta, 2009, 79(3): 900-904.

[7] Fan Y Q(范艳群), Chen Q Y(陈庆阳), Xia J M(夏金梅), et al. Detection of glucosamine hydrochloride by ion chromatography with integrated pulsed amperometric detector [J]. Journal of Electrochemistry(电化学), 2014, 20(2): 164-170.

[8] Freitas C B, Moreira R C, de Oliveira Tavares M G, et al. Monitoring of nitrite, nitrate, chloride and sulfate in environmental samples using electrophoresis microchips coupled with contactless conductivity detection[J]. Talanta, 2016, 147: 335-341.

[9] Butt S B, Riaz M, Iqbal M Z. Simultaneous determination of nitrite and nitrate by normal phase ion-pair liquid chromatography[J]. Talanta, 2001, 55(4): 789-797.

[10] Wang C Y(王春燕), Liu X Q(刘晓秋), Qi Y X(戚颖欣). Electrochemical detection of hydrogen peroxide at AuNPs modified electrode using p-hydroxyphenylboronic acid as a precursor[J]. Journal of Electrochemistry(电化学), 2016, 22(1): 88-93.

[11] Shi P(石鹏), Wang B X(王伯轩), Song Q L(宋泉霖), et al. Application of Pd/graphene modified electrode in the detection of 4-chlorophenol[J]. Journal of Electrochemistry(电化学), 2015, 21(5): 488-495.

[12] Oyama S T, Gott T, Zhao H, et al. Transition metal phosphide hydroprocessing catalysts: A review[J]. Catalysis Today, 2009, 143(1/2): 94-107.

[13] Carenco S, Portehault D, Boissiere C, et al. Nanoscaled metal borides and phosphides: recent developments and perspectives[J]. Chemical Reviews, 2013, 113(10): 7981-8065.

[14] Wang H J(王慧娟). Synthesis of ultrathin Co_3O_4 nanoflakes film material for electrochemical sensing[J]. Journal of Electrochemistry(电化学), 2016, 22(6): 631-635.

[15] Tang C, Cheng N Y, Pu Z H, et al. NiSe nanowire film supported on nickel foam: an efficient and stable 3D bifunctional electrode for full water splitting[J]. Angewandte Chemie International Edition, 2015, 127 (32): 9483-9487.

[16] Jiang P, Liu Q, Liang Y H, et al. A cost-effective 3D hydrogen evolution cathode with high catalytic activity: FeP nanowire array as the active phase[J]. Angewandte Chemie International Edition, 2014, 126(47): 13069-13073.

[17] Li M X(李明轩), Ou J L(欧洁连), Chen Y X(陈燕鑫), et al. Preparation and catalytic properties of FeCo alloy nanocatalyst[J]. Journal of Electrochemistry(电化学), 2013, 19(2): 125-129.

[18] Liu Y W, Cao X Q, Kong R M, et al. Cobalt phosphide nanowire array as an effective electrocatalyst for non-enzymatic glucose sensing[J]. Journal of Materials Chemistry B, 2017, 5(10): 1901-1904.

[19] Tian J Q, Liu Q, Asiri A M, et al. Self-supported nanoporous cobalt phosphide nanowire arrays: an efficient 3D hydrogen-evolving cathode over the wide range of pH 0-14[J]. Journal of the American Chemical Society, 2014, 136(21): 7587-7590.

[20] Liu T T, Wang K Y, Du G, et al. Self-supported CoP nanosheet arrays: a non-precious metal catalyst for efficient hydrogen generation from alkaline $NaBH_4$ solution [J]. Journal of Materials Chemistry A, 2016, 4(34): 13053-13057.

[21] Ai L, Niu Z, Jiang J. Mechanistic insight into oxygen evolution electrocatalysis of surface phosphate modified cobalt phosphide nanorod bundles and their superior performance for overall water splitting[J]. Electrochimica Acta, 2017, 242: 355-363.

[22] Pham X H, Li C A, Han K N, et al. Electrochemical detection of nitrite using urchin-like palladium nanostructures on carbon nanotube thin film electrodes[J]. Sensors and Actuators B: Chemical, 2014, 193: 815-822.

[23] Radhakrishnan S, Krishnamoorthy K, Sekar C, et al. A highly sensitive electrochemical sensor for nitrite detection based on Fe_2O_3 nanoparticles decorated reduced graphene oxide nanosheets[J]. Applied Catalysis B: Environmental, 2014, 148: 22-28.

[24] Zhang D, Fang Y X, Miao Z Y, et al. Direct electrodeposion of reduced graphene oxide and dendritic copper nanoclusters on glassy carbon electrode for electrochemical detection of nitrite[J]. Electrochimica Acta, 2013, 107: 656-663.

[25] Wang P, Mai Z B, Dai Z, et al. Construction of Au nanoparticles on choline chloride modified glassy carbon electrode for sensitive detection of nitrite[J]. Biosensors and Bioelectronics, 2009, 24(11): 3242-3247.

[26] Shahid M M, Rameshkumar P, Pandikumar A, et al. An electrochemical sensing platform based on a reduced graphene oxide-cobalt oxide nanocube@platinum nanocomposite for nitric oxide detection[J]. Journal of Materials Chemistry A, 2015, 3(27): 14458-14468.

[27] Ting S L, Guo C X, Leong K C, et al. Gold nanoparticles decorated reduced graphene oxide for detecting the presence and cellular release of nitric oxide[J]. Electrochimica Acta, 2013, 111: 441-446.

[28] Pandikumar A, Yusoff N, Huang N M, et al. Electrochemical sensing of nitrite using a glassy carbon elec-

trode modified with reduced functionalized graphene oxide decorated with flower-like zinc oxide[J]. Microchimica Acta, 2015, 182(5/6): 1113-1122.

[29] Haldorai Y, Kim J Y, Vilian A T E, et al. An enzyme-free electrochemical sensor based on reduced graphene oxide/Co_3O_4 nanospindle composite for sensitive detection of nitrite[J]. Sensors and Actuators B: Chemical, 2016, 227: 92-99.

[30] Saravanan J, Ramasamy R, Therese H A, et al. Electrospun CuO/NiO composite nanofibers for sensitive and selective non-enzymatic nitrite sensors[J]. New Journal of Chemistry, 2017, 41(23): 14766-14771.

[31] Lu L. Highly sensitive detection of nitrite at a novel electrochemical sensor based on mutually stabilized Pt nanoclusters doped CoO nanohybrid[J]. Sensors and Actuators B: Chemical, 2019, 281: 182-190.

[32] Wu Y Y, Li C, Dou Z Y, et al. A novel nitrite sensor fabricated through anchoring nickel-tetrahydroxy-phthalocyanine and polyethylene oxide film onto glassy carbon electrode by a two-step covalent modification approach [J]. Journal of Solid State Electrochemistry, 2014, 18(9): 2625-2635.

[33] Mani V, Periasamy A P, Chen S M. Highly selective amperometric nitrite sensor based on chemically reduced graphene oxide modified electrode[J]. Electrochemistry Communications, 2012, 17: 75-78.

High-Efficiency Nitrite Sensor Based on CoP Nanowire Array

ZHOU Fu-ling[1,2], XIONG Xiao-li[2*], SUN Xu-ping[1*]

(1. *Institute of Fundamental and Frontier Sciences, University of Electronic Science and Technology of China, Chengdu* 610054, *Sichuan, China*; 2. *College of Chemistry and Material Science, Sichuan Normal University, Chengdu* 610068, *Sichuan, China*)

Abstract: Nitrite has a negative impact on the environment and human health. The long-term consumption of nitrite-containing foods has a carcinogenic risk. Therefore, the analysis and detection of nitrite are important. It is of great significance to develop high-efficiency electrocatalysts to achieve high sensitivity and selectivity for nitrite detection. The cobalt phosphide nano-array (CoP/TM) was obtained by hydrothermal and low-temperature phosphating. The electrochemical test results show that the constructed CoP/TM was a highly efficient electrochemical reduction nitrite catalyst with the excellent sensing performance and response time less than 3 s, as well as the linear detection range of 1.0 μmol·L^{-1} to 1.0 mmol·L^{-1} and lower detection limit of 18 nmol·L^{-1} (S/N = 3). The response sensitivity was 17718 μA·(mmol·L^{-1})$^{-1}$·cm^{-2} with the satisfactory selectivity.

Key words: CoP; nanoarray; nitrite; electrochemistry; sensor